Progress In Electromagnetics Research, PIER 52, 1–21, 2005

ELLIPTICAL AND CIRCULAR STEP-INDEX FIBERS WITH CONDUCTING HELICAL WINDINGS ON THE CORE-CLADDING BOUNDARIES FOR DIFFERENT WINDING PITCH ANGLES — A COMPARATIVE MODAL DISPERSION ANALYSIS

D. Kumar

Department of Applied Physics
Delhi College of Engineering
Delhi-110042, India

O. N. Singh II

Department of Applied Physics
Institute of Technology
Banaras Hindu University, Varanasi-221 005, India

Abstract—The propagation characteristics of an elliptical step-index fiber with a conducting helical winding on the core-cladding boundary are investigated analytically and compared with those of a circular step index fiber with a conducting radial winding. Our optical waveguides are unconventional: in view of the existence of helical conducting windings on the core-cladding boundaries. Appropriate coordinate systems, circular cylindrical and elliptic cylindrical, are chosen for the circular and elliptical fibers. Applying the boundary conditions as modified by the presence of conducting helical windings, the characteristic equations are obtained for both the fibers. Dispersion curves are also obtained for two special values of the helical pitch angle ψ, namely, for $\psi = 0^\circ$ and $\psi = \frac{\pi}{2}$ for each fiber and the results have been compared. It is found that the introduction of the helical winding has two main effects on the characteristics of both types of fibers. These are: (1) The helix introduces band gaps and (2) has the effect of splitting a mode into a pair of adjacent modes In the case of the elliptical helically clad waveguide we find two band gaps for $V < 30$ whereas for circular guide we have only one band gap in the same range of V-values, V being the normalized frequency parameter.

1 Introduction

2 Theoretical Analysis

3 Boundary Conditions

4 Characteristic Equation

4.1 Circular Step-Index Fiber

4.2 Elliptical Step-Index Fiber

5 Results and Discussion

Acknowledgment

References

1. INTRODUCTION

Optical waveguides have been investigated extensively during the past four decades [1–4]. Considerable research has been done on optical fibers with more general geometries than that of the standard step index circular fiber and various refractive-index profiles have also been studied [5–7]. As is well known, researchers have concentrated on circular and rectangular waveguides, and Chu [8] directed his attention to elliptic waveguides. Chu was followed by Dyott and Stern [9] who analyzed elliptic fibers. Later the propagation characteristics of optical fibers with elliptical cross sections and circular cross sections were investigated by numerous researchers. Singh et al. [10] proposed an analytical study of the dispersion characteristics of a circular step-index optical fiber with a helical conducting winding on the core-cladding boundary. The case of an elliptical step-index fiber with a helical conducting winding on the core-cladding interface was first studied by Deepak Kumar and O. N. Singh II [11]. Here we propose to compare an elliptic core optical fiber and circular core optical fiber with a conducting sheath helix [12] between the core and the cladding regions Fig. 1(a). Although we present the analysis for the general case when there is no restriction on ψ, but for simplicity we have considered only two particular helical pitch angles, $\psi = 0^\circ$ and $\psi = \frac{\pi}{2}$.

The sheath helix is a cylindrical surface with high conductivity in a preferential direction which winds helically at constant angle (pitch angle ψ) around the core-cladding boundary surface. In our waveguides the core and the cladding regions are assumed to have constant real refractive indices n_1 and n_2 ($n_1 > n_2$) and the fibers are referred to as the elliptical helically cladded fiber (EHCF), and the circular helically cladded fiber (CHCF). The pitch angle ψ can be used for controlling

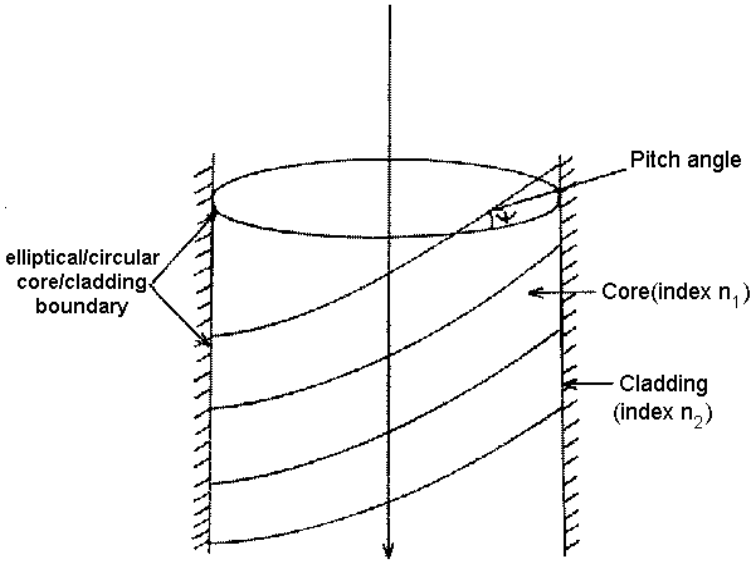

Figure 1a.

the modal behaviour of such fibers. This additional control parameter may prove important for technology in the near future.

The description of a sheath helix is given in Watkins [14]. A sheath helix can be approximated in practice by winding a very thin conducting wires around the cylindrical surface so that the spacing between the adjacent windings is very small and yet they are insulate from one another. Thus in Fig. 1(e), $d > w$ and both are very small, and in the limit both tend to zero Fig. 1(b). An alternative way of realizing the sheath is to have a thin planar sheet made of alternate conducting thin strips and non conducting gaps-obliquely and then wrapping it along the cylindrical core without overlap Fig. 1(c). The cladding material (n_2) is next to be deposited cylindrically around the core with the winding. It is to be admitted that on the microscopic scale the manufacture of such structure will present difficulties; but these may not be insurmountable in the present age of nanotechnology.

Due to the complexities of a helical geometry the mathematical steps become very difficult and some suitable approximations [2] are made in case of the elliptical fiber. In case of the circular fiber, however no approximations are needed. The use of Mathieu functions, modified Mathieu functions [15], Bessel functions, modified Bessel functions [16] have been made. Due to mathematical difficulties we take up two

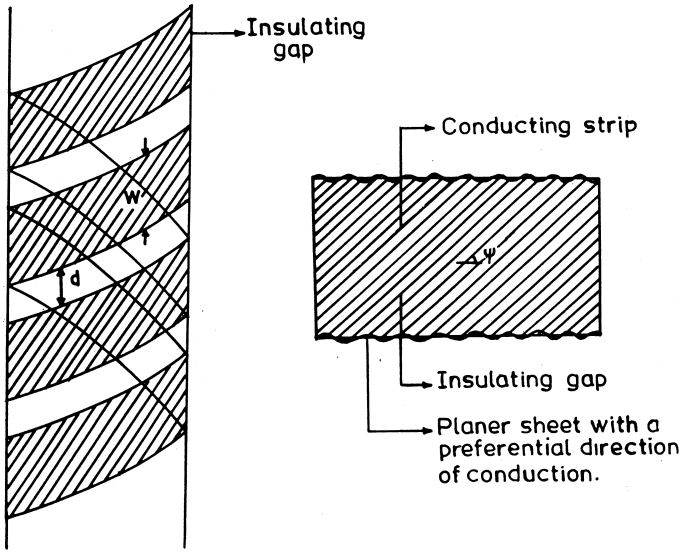

Figure 1b. Sheath helix (magnified). **Figure 1c.**

simple special cases: namely $\psi = 0°$ and $\psi = \frac{\pi}{2}$.

We choose $n_1 > n_2$ and assume that

$$\frac{n_1 - n_2}{n_1} \ll 1$$

This means that we are using the scalar wave weak guidance approximation. However, in applying the boundary conditions we preserve the vector nature of the fields.

We introduce coordinates (r, ϕ, z) and (ξ, η, z) for the circular [17] and the elliptical [17] fibers respectively.

The fibers of circular and elliptical cross-sections are shown in Fig. 1(a).

2. THEORETICAL ANALYSIS

We give the expressions for field components of circular step-index fiber [11–13] and the elliptical step index fiber [2] in Table 1.

In Table 1 we have

$$k^2 n_1^2 - \beta^2 = k_1^2 = u^2$$
$$\beta^2 - k^2 n_2^2 = k_2^2 = w^2$$

Table 1.

Field Components (Circular step-index fiber)	Field Components (Elliptical step-index fiber)
$Ez_1 = AJ_v(k_1r)e^{i(\omega t-\beta z+v\phi)}$ (1)	$Ez_1 = \sqrt{\frac{\mu_0}{\epsilon_1}}\, B'Se_v\ (\xi,\gamma_1^2)\sin v\eta$ (1A)
$Hz_1 = BJ_v(k_1r)e^{i(\omega t-\beta z+v\phi)}$ (2)	$Ez_2 = \sqrt{\frac{\mu_0}{\epsilon_2}}\, PGek_v\ (\xi,-\gamma_2^2)\sin v\eta$ (2A)
$Ez_2 = CK_v(k_2r)e^{i(\omega t-\beta z+v\phi)}$ (3)	$Hz_1 = A'Ce_v(\xi,\gamma_1^2)\cos v\eta$ (3A)
$Hz_2 = DK_v(k_2r)e^{i(\omega t-\beta z+v\phi)}$ (4)	$Hz_2 = LFek_v(\xi,-\gamma_2^2)\cos v\eta$ (4A)
$E\phi_1 = -\frac{i}{k_1^2}\big[\frac{iv\beta}{r}AJ_v(k_1r)$ $-\omega\mu_0k_1BJ_v'(k_1r)\big]e^{i(\omega t-\beta z+v\phi)}$ (5)	$E\eta_1 = \frac{i}{(k^2n_1^2-\beta^2)q\ell}[\beta B'Se_v(\xi,\gamma_1^2)$ $\cdot\cos v\eta v-\omega\mu_0A'Ce_v'(\xi,\gamma_1^2)\cos v\eta]$ (5A)
$H\phi_1 = -\frac{i}{k_1^2}\big[\frac{iv\beta}{r}BJ_v(k_1r)$ $+\omega\epsilon_1k_1AJ_v'(k_1r)\big]e^{i(\omega t-\beta z+v\phi)}$ (6)	$E\eta_2 = \frac{i}{(k^2n_2^2-\beta^2)q\ell}[\beta PGek_v(\xi,-\gamma_2^2)$ $\cdot\cos v\eta v-\omega\mu_0LFek_v'(\xi,-\gamma_2^2)\cos v\eta]$ (6A)
$E\phi_2 = -\frac{i}{k_2^2}\big[\frac{iv\beta}{r}CK_v(k_2r)$ $-\omega\mu_0k_2DK_v'(k_2r)\big]e^{i(\omega t-\beta z+v\phi)}$ (7)	$H\eta_1 = \frac{i}{(k^2n_1^2-\beta^2)q\ell}[\beta A'Ce_v(\xi,\gamma_1^2)(-\sin v\eta)v$ $+\omega n_1^2\epsilon_0B'Se_v'(\xi,\gamma_1^2)\sin v\eta]$ (7A)
$H\phi_2 = -\frac{i}{k_2^2}\big[\frac{iv\beta}{r}DK_v(k_2r)$ $+\omega\epsilon_2k_2CK_v'(k_2r)\big]e^{i(\omega t-\beta z+v\phi)}$ (8)	$H\eta_2 = \frac{i}{(k^2n_1^2-\beta^2)q\ell}[\beta LFek_v(\xi,-\gamma_2^2)(-\sin v\eta)v$ $+\omega n_2^2\epsilon_0PGek_v'(\xi,-\gamma_2^2)\sin v\eta]$ (8A)

and $\ell = (\cosh^2\xi - \cos^2\eta)^{1/2}$. Here $k = \frac{2\pi}{\lambda}$, λ being the operating wavelength and β is the propagation constant for the guided waves.

Here

$$\begin{aligned}
\gamma_1^2 &= \frac{\left(n_1^2k^2-\beta^2\right)q^2}{4}\\
\Rightarrow \gamma_1^2 &= \frac{u^2q^2}{4}\\
\Rightarrow \gamma_1 &= \frac{uq}{2}\\
\gamma_2^2 &= \frac{\left(\beta^2-n_2^2k^2\right)q^2}{4}\\
\Rightarrow \gamma_2^2 &= \frac{w^2q^2}{4}\\
\Rightarrow \gamma_2 &= \frac{wq}{2}
\end{aligned}$$

Also, $Se_v(\xi,\gamma_1^2)$ and $Ce_v(\xi,\gamma_1^2)$ are the modified Mathieu functions of the first kind, and $Gek_v(\xi,-\gamma_2^2)$ and $Fek_v(\xi,-\gamma_2^2)$ are the modified

Mathieu functions of the second kind.

$Se'_v(\xi, \gamma_1^2)$ and $Ce'_v(\xi, \gamma_1^2)$ are the first derivatives of the modified Mathieu functions of the first kind, and $Gek'_v(\xi, -\gamma_2^2)$ and $Fek'_v(\xi, -\gamma_2^2)$ are the first derivatives of the modified Mathieu functions of the second kind.

3. BOUNDARY CONDITIONS

We are concerned with only ϕ, z and ξ, z in writing the boundary conditions [11] for a conducting helix wound around the circular core-cladding boundary and the elliptic core-cladding boundary respectively. Remembering that the tangential component of the electric field in the direction of the conducting helix should be zero, and in the direction perpendicular to the helical winding, the tangential component of both the electric and magnetic field must be continuous, we have the following eight boundary conditions:

Table 2.

Boundary conditions (Circular step-index fiber)		Boundary conditions (Elliptical step-index fiber)	
$Ez_1 \sin\psi + E\phi_1 \cos\psi = 0$	(9)	$Ez_1 \sin\psi + E\eta_1 \cos\psi = 0$	(9A)
$Ez_2 \sin\psi + E\phi_2 \cos\psi = 0$	(10)	$Ez_2 \sin\psi + E\eta_2 \cos\psi = 0$	(10A)
$(Ez_1 - Ez_2)\cos\psi - (E\phi_1 - E\phi_2)\sin\psi = 0$	(11)	$(Ez_1 - Ez_2)\cos\psi - (E\eta_1 - E\eta_2)\sin\psi = 0$	(11A)
$(Hz_1 - Hz_2)\sin\psi + (H\phi_1 - H\phi_2)\cos\psi = 0$	(12)	$(Hz_1 - Hz_2)\sin\psi + (H\eta_1 - H\eta_2)\cos\psi = 0$	(12A)

One may ask why we use the boundary conditions as described by equations (9)–(12) and equations (9A)–(12A) on the entire boundary surface when the conducting regions alternate with insulating regions. Indeed, if we did not make this plausible approximation, the mathematical steps would be formidably complicated. As a justification for this simplifying approximation we may say that, in the first place, we may choose $w > d$, so that the gaps are of infinitesimal width, and secondly under the weak guidance approximation $\frac{n_1 - n_2}{n_1} \ll 1$, so that $n_1 \approx n_2$. In the gaps, therefore the boundary between the core and the cladding becomes less and less pronounced as $n_1 - n_2 \to 0$. However, if $n_1 - n_2$ is substantially large, for a strict analysis one has to use Table 2 for the conducting region and Table 3 for the insulating dielectric region. In the absence of the conducting helical windings the boundary conditions would have been made as in Table 3.

Table 3.

Ordinary boundary conditions (Circular step-index fiber) without helix	Ordinary boundary conditions (Elliptical step-index fiber) without helix
$Ez_1 = Ez_2$	$Ez_1 = Ez_2$
$Hz_1 = Hz_2$	$Hz_1 = Hz_2$
$E\phi_1 = E\phi_2$	$E\eta_1 = E\eta_2$
$H\phi_1 = H\phi_2$	$H\eta_1 = H\eta_2$

4. CHARACTERISTIC EQUATION

4.1. Circular Step-Index Fiber

Substituting the expressions for Ez_1, Hz_1, Ez_2, Hz_2, $E\phi_1$, $H\phi_1$, $E\phi_2$ and $H\phi_2$ from equations (1)–(8) in equations (9)–(12), we get

$$\left(\sin\psi + \frac{v\beta}{au^2}\cos\psi\right) AJ_v(k_1a) + \frac{i\omega\mu_0}{u} BJ'_v(k_1a)\cos\psi = 0 \quad (13)$$

$$\left(\sin\psi + \frac{v\beta}{aw^2}\cos\psi\right) CK_v(k_2a) + \frac{i\omega\mu_0}{w} D\cos\psi K'_v(k_2a) = 0 \quad (14)$$

$$\left(\cos\psi - \frac{v\beta}{au^2}\sin\psi\right) AJ_v(k_1a) - \frac{i\omega\mu_0}{u}\sin\psi BJ'_v(k_1a)$$
$$- \left(\cos\psi - \frac{v\beta}{aw^2}\sin\psi\right) CK_v(k_2a) + \frac{i\omega\mu_0}{w}\sin\psi DK'_v(k_2a) = 0 \quad (15)$$

$$-\frac{i\omega\epsilon_1}{u} AJ'_v(k_1a)\cos\psi + \left(\sin\psi + \frac{v\beta}{au^2}\cos\psi\right) BJ_v(k_1a)$$
$$+\frac{i\omega\epsilon_2}{w} CK'_v(k_2a)\cos\psi - \left(\sin\psi + \frac{v\beta}{aw^2}\cos\psi\right) DK_v(k_2a) = 0 \quad (16)$$

Eliminating A, B, C and D from equations (13)–(16), we get

$$\begin{vmatrix} (\sin\psi + \frac{v\beta}{au^2}\cos\psi)J_v(k_1a) & \frac{i\omega\mu_0}{u}J_v'(k_1a)\cos\psi & 0 & 0 \\ 0 & 0 & (\sin\psi + \frac{v\beta}{aw^2}\cos\psi)K_v(k_2a) & \frac{i\omega\mu_0}{w}K_v'(k_2a)\cos\psi \\ (\cos\psi - \frac{v\beta}{au^2}\sin\psi)J_v(k_1a) & -\frac{i\omega\mu_0}{u}\sin\psi J_v'(k_1a) & -(\cos\psi - \frac{v\beta}{aw^2}\sin\psi)K_v(k_2a) & \frac{i\omega\mu_0}{w}\sin\psi K_v'(k_2a) \\ -\frac{i\omega\epsilon_1}{u}J_v'(k_1a)\cos\psi & (\sin\psi + \frac{v\beta}{au^2}\cos\psi)J_v(k_1a) & \frac{i\omega\epsilon_2}{w}K_v'(k_2a)\cos\psi & -(\sin\psi + \frac{v\beta}{aw^2}\cos\psi)K_v(k_2a) \end{vmatrix} = 0 \quad (17)$$

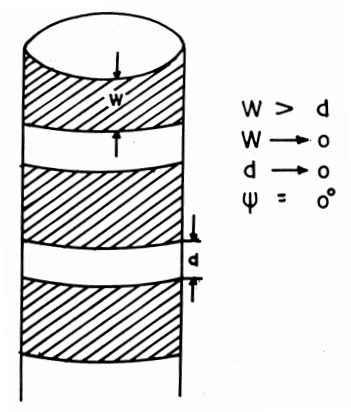

Figure 1d. Periodicity of spatial structure persists.

Now we are going to take two special cases for the circular step-index fiber, namely $\psi = 0°$, (Case I) and $\psi = \frac{\pi}{2}$ (Case II). We can visualize the geometrical situations by looking at Fig. 1(d) and Fig. 1(e). The periodicity in the propagation direction (axial direction) remains because even when $\psi = 0°$, the structural feature repeats after a spatial interval of $d + w$.

When $\psi = \frac{\pi}{2}$, the periodicity remains in the circumferential direction, but as the propagation takes place in the axial direction, the circumferential periodicity is not expected to introduce band gaps. We can now consider the analysis of Case I and Case II.

Case I: We set $\psi = 0°$ and $v = 1$ in the determinantal eq. (17) and expand it, we get

$$\begin{aligned}
&\frac{\beta^2}{a^2u^3}J_1^2K_1\left(-\frac{K_1}{w}-K_0\right)-\frac{\beta^2}{a^2w^3}\left(-\frac{J_1^2K_1^2}{u}+J_0J_1K_1^2\right)\\
&\quad-\frac{\frac{4\pi^2}{\lambda^2}n_2^2}{w}\left(-\frac{J_1^2}{u}+J_0J_1\right)\left(\frac{K_1^2}{w^2}+K_0^2+2K_0\frac{K_1}{w}\right)\\
&\quad-\frac{\frac{4\pi^2}{\lambda^2}n_1^2}{u}\left(\frac{J_1^2}{u^2}+J_0^2-\frac{2J_1}{u}J_0\right)\left(-\frac{K_1^2}{w}-K_0K_1\right)\;=\;0 \quad (18)
\end{aligned}$$

Case II: We set $\psi = \frac{\pi}{2}$ and $v = 1$ in the determinantal eq. (17) and

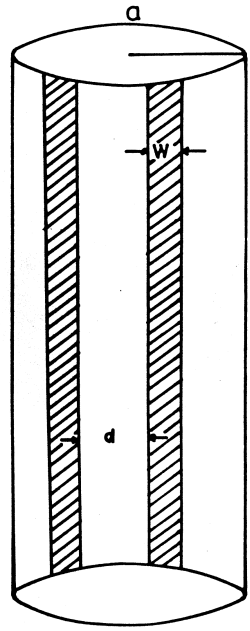

Figure 1e. $d > w,\ w \to 0,\ d \to 0,\ \psi = \pi/2$. Nonaxial periodicity only circumferential periodicity. Total number of conducting strips $N = \frac{2\pi a}{w+d}$.

expand it. Then we have

$$-\frac{J_1K_1 + uJ_0K_1}{u^2} + \frac{J_1K_1 + wJ_1K_0}{w^2} = 0 \tag{19}$$

The dispersion curves corresponding to eq. (18) are shown in the Fig. 2. The dispersion curves corresponding to eq. (19) are shown in the Fig. 3.

4.2. Elliptical Step-Index Fiber

Substituting the expressions for Ez_1, Hz_1, Ez_2, Hz_2, $E\eta_1$, $H\eta_1$, $E\eta_2$ and $H\eta_2$ from equations (1A)–(8A) in equations (9A)–(12A), we get

$$A'\frac{i}{u^2q\ell}\omega\mu_0 Ce'_v(\xi,\gamma_1^2)\cos v\eta\cos\psi$$
$$-B'\left[\sqrt{\frac{\mu_0}{\epsilon_1}}Se_v(\xi,\gamma_1^2)\sin v\eta\sin\psi + \frac{i}{u^2q\ell}\beta Se_v(\xi,\gamma_1^2)\cos v\eta v\right] = 0 \tag{20}$$

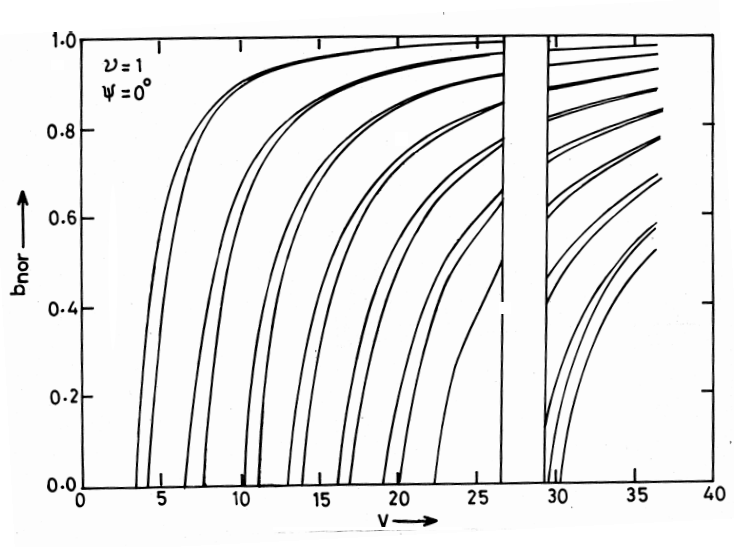

Figure 2. Dispersion curves (normalized frequency versus normalized propagation constant) for $\psi = 0°$ in the case of the circular step-index fiber.

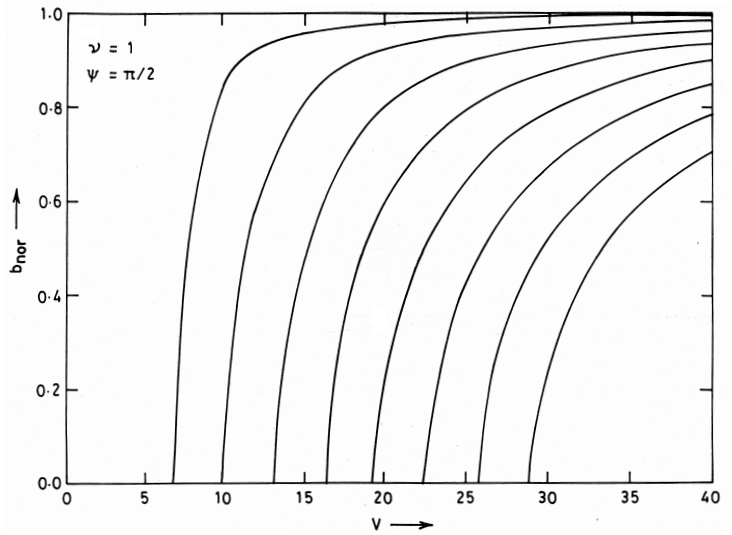

Figure 3. Dispersion curves (normalized frequency versus normalized propagation constant) for $\psi = \pi/2$ in the case of the circular step-index fiber.

$$P\left[\sqrt{\frac{\mu_0}{\epsilon_2}}Gek_v(\xi,-\gamma_2^2)\sin v\eta\sin\psi-\frac{i\beta}{w^2q\ell}Gek_v(\xi,-\gamma_2^2)\cos v\eta v\cos\psi\right]$$
$$+L\frac{i\omega\mu_0}{w^2q\ell}Fek_v'(\xi,-\gamma_2^2)\cos v\eta\cos\psi=0 \quad (21)$$

$$A'\frac{i\omega\mu_0}{u^2q\ell}Ce_v'(\xi,\gamma_1^2)\cos v\eta\sin\psi$$
$$+B'\left[\sqrt{\frac{\mu_0}{\epsilon_1}}Se_v(\xi,\gamma_1^2)\sin v\eta\cos\psi-\frac{i}{u^2q\ell}\beta Se_v(\xi,\gamma_1^2)\cos v\eta v\sin\psi\right]$$
$$-P\left[\sqrt{\frac{\mu_0}{\epsilon_2}}Gek_v(\xi,-\gamma_2^2)\sin v\eta\cos\psi-\frac{i\beta}{w^2q\ell}Gek_v(\xi,-\gamma_2^2)\cos v\eta v\sin\psi\right]$$
$$-L\frac{i\omega\mu_0}{w^2q\ell}Fek_v'(\xi,-\gamma_2^2)\cos v\eta\sin\psi=0 \quad (22)$$

$$A'\left[Ce_v(\xi,\gamma_1^2)\cos v\eta\sin\psi-\frac{i\beta}{u^2q\ell}Ce_v(\xi,\gamma_1^2)\sin v\eta v\cos\psi\right]$$
$$+B'\frac{i\omega n_1^2\epsilon_0}{u^2q\ell}Se_v'(\xi,\gamma_1^2)\sin v\eta\cos\psi$$
$$+P\frac{i}{w^2q\ell}\omega n_2^2\epsilon_0Gek_v'(\xi,-\gamma_2^2)\sin v\eta\cos\psi$$
$$-L\left[Fek_v(\xi,-\gamma_2^2)\cos v\eta\sin\psi+\frac{i\beta}{w^2q\ell}Fek_v(\xi,-\gamma_2^2)\sin v\eta v\cos\psi\right]$$
$$=0 \quad (23)$$

where

$$k^2n_1^2-\beta^2 \;=\; k_1^2=u^2$$

$$\beta^2-k^2n_2^2 \;=\; k_2^2=w^2$$

and

$$\ell=(\cosh^2\xi-\cos^2\eta)^{1/2}.$$

Eliminating A', B', P and L from equations (20)–(23) at $\xi=\xi_0$ we get

$$
\begin{vmatrix}
\dfrac{i}{w^2q\ell}\omega\mu_0 Ce'_v(\xi_0,\gamma_1^2) & -[\sqrt{\dfrac{\mu_0}{\epsilon_1}}Se_v(\xi_0,\gamma_1^2)\sin v\eta\sin\psi & 0 & 0 \\
\cdot\cos v\eta\cos\psi & +\dfrac{i}{w^2q\ell}\beta Se_v(\xi_0,\gamma_1^2)\cos v\eta v\cos\psi] & & \\
0 & 0 & [\sqrt{\dfrac{\mu_0}{\epsilon_2}}Gek_v(\xi_0,-\gamma_2^2)\sin v\eta\sin\psi & \dfrac{i\omega\mu_0}{w^2q\ell}Fek'_v(\xi_0-\gamma_2^2)\cos v\eta\cos\psi \\
 & & +\dfrac{i\beta}{w^2q\ell}Gek_v(\xi_0,-\gamma_2^2)\cos v\eta v\cos\psi] & \\
\dfrac{i\omega\mu_0}{w^2q\ell}Ce'_v(\xi,\gamma_1^2)\cos v\eta\sin\psi & [\sqrt{\dfrac{\mu_0}{\epsilon_1}}Se_v(\xi_0,\gamma_1^2)\sin v\eta\cos\psi & -[\sqrt{\dfrac{\mu_0}{\epsilon_2}}Gek_v(\xi_0,-\gamma_2^2)\sin v\eta\cos\psi & -\dfrac{i\omega\mu_0}{w^2q\ell}Fek'_v(\xi_0,-\gamma_2^2)\cos v\eta\sin\psi \\
 & -\dfrac{i}{w^2q\ell}\beta Se_v(\xi_0,\gamma_1^2)\cos v\eta v\sin\psi] & -\dfrac{i\beta}{w^2q\ell}Gek_v(\xi_0,-\gamma_2^2)\cos v\eta v\sin\psi] & \\
[Ce_v(\xi_0,\gamma_1^2)\cos v\eta\sin\psi & \dfrac{i\omega n_1^2\epsilon_0}{w^2q\ell}Se'_v(\xi_0,\gamma_1^2)\sin v\eta\cos\psi & \dfrac{i}{w^2q\ell}\omega n_2^2\epsilon_0 Gek'_v(\xi_0,-\gamma_2^2)\sin v\eta\cos\psi & -[Fek_v(\xi_0,-\gamma_2^2)\cos v\eta\sin\psi \\
-\dfrac{i\beta}{w^2q\ell}Ce_v(\xi_0,\gamma_1^2)\sin v\eta v\cos\psi] & & & +\dfrac{i\beta}{w^2q\ell}Fek_v(\xi_0,-\gamma_2^2)\sin v\eta v\cos\psi]
\end{vmatrix} = 0 \tag{24}
$$

Again we are going to take two special cases for elliptical step-index fiber also.

Case I: When $\psi = 0^\circ$ and $v = 1$ in determinantal (24) and expand it, we get

$$\begin{aligned} U^2k^2n_2^2\frac{Ce_1'(\xi_0,\gamma_1^2)}{Ce_1(\xi_0,\gamma_1^2)}\frac{Fek_1'(\xi_0,-\gamma_2^2)}{Fek_1(\xi_0,-\gamma_2^2)}\frac{Gek_1'(\xi_0,-\gamma_2^2)}{Gek_1(\xi_0,-\gamma_2^2)} \\ -W^2k^2n_1^2\frac{Ce_1'(\xi_0,\gamma_1^2)}{Ce_1(\xi_0,\gamma_1^2)}\frac{Se_1'(\xi_0,\gamma_1^2)}{Se_1(\xi_0,\gamma_1^2)}\frac{Fek_1'(\xi_0,-\gamma_2^2)}{Fek_1(\xi_0,-\gamma_2^2)} \\ -U^2\beta^2\frac{Ce_1'(\xi_0,\gamma_1^2)}{Ce_1(\xi_0,\gamma_1^2)}+W^2\beta^2\frac{Fek_1'(\xi_0,-\gamma_2^2)}{Fek_1(\xi_0,-\gamma_2^2)} \;=\; 0 \end{aligned} \tag{25}$$

where $U = ua$ and $W = wa$.

We apply the approximations [2] as given below.

The approximations are

$$\frac{Ce_1'(\xi_0,\gamma_1^2)}{Ce_1(\xi_0,\gamma_1^2)} \approx u(1-e^2)^{1/2}\left[\frac{J_1'(u_e)+\left(\frac{u^2e^2}{32}\right)J_3'(u_e)}{J_1(u_e)+\left(\frac{u^2e^2}{32}\right)J_3(u_e)}\right] \tag{26a}$$

$$\frac{Se_1'(\xi_0,\gamma_1^2)}{Se_1(\xi_0,\gamma_1^2)} \approx \frac{e^2}{(1-e^2)^{1/2}}+u(1-e^2)^{1/2}\left[\frac{J_1'(u_e)+\left(\frac{3u^2e^2}{32}\right)J_3'(u_e)}{J_1(u_e)+\left(\frac{3u^2e^2}{32}\right)J_3(u_e)}\right] \tag{26b}$$

$$\frac{Fek_1'(\xi_0,-\gamma_2^2)}{Fek_1(\xi_0,-\gamma_2^2)} \approx w(1-e^2)^{1/2}\left[\frac{K_1'(w_e)+\left(\frac{w^2e^2}{32}\right)K_3'(w_e)}{K_1(w_e)+\left(\frac{w^2e^2}{32}\right)K_3(w_e)}\right] \tag{26c}$$

$$\frac{Gek_1'(\xi_0,-\gamma_2^2)}{Gek_1(\xi_0,-\gamma_2^2)} \approx \frac{e^2}{(1-e^2)^{1/2}}+w(1-e^2)^{1/2}\left[\frac{K_1'(w_e)+\left(\frac{3w^2e^2}{32}\right)K_3'(w_e)}{K_1(w_e)+\left(\frac{3w^2e^2}{32}\right)K_3(w_e)}\right] \tag{26d}$$

In equations (26a)–(26d) e is the eccentricity of the ellipse

$$e = 1 - \left(\frac{b}{a}\right)^2 = \text{sech}^2\xi_0.$$

u_e and w_e are arguments of Bessel functions

$$\begin{aligned} u_e &= 2Y_1 \cosh\xi_0 \\ w_e &= 2Y_2 \cosh\xi_0 \end{aligned}$$

where Y_1 and Y_2 are given in page 5.

Applying the above approximations from eqs. (26a)–(26d) in eq. (25), we get

$$uwa^2(1-e^2)\left\{\frac{J_1'(U)+\dfrac{u^2a^2e^2}{32}J_3'(U)}{J_1(U)+\left(\dfrac{u^2a^2e^2}{32}\right)J_3(U)}\right\}\left\{\frac{K_1'(W)+\dfrac{w^2a^2e^2}{32}K_3'(W)}{K_1(W)+\dfrac{w^2a^2e^2}{32}K_3(W)}\right\}$$

$$\cdot\left(\frac{2\pi}{\lambda}\right)^2\left[\left\{\frac{e^2}{(1-e^2)^{1/2}}+wa(1-e^2)^{1/2}\left(\frac{K_1'(W)+\dfrac{3w^2a^2e^2}{32}K_3'(W)}{K_1(W)+\dfrac{3w^2a^2e^2}{32}K_3(W)}\right)\right\}\right.$$

$$\cdot u^2a^2n_2^2+\left\{\frac{e^2}{(1-e^2)^{1/2}}+ua(1-e^2)^{1/2}\left(\frac{J_1'(U)+\dfrac{3u^2a^2e^2}{32}J_3'(U)}{J_1(U)+\dfrac{3u^2a^2e^2}{32}J_3(U)}\right)\right\}$$

$$\left.\cdot w^2a^2n_1^2\right]-ua(1-e^2)^{1/2}\left(\frac{J_1'(U)+\dfrac{u^2a^2e^2}{32}J_3'(U)}{J_1(U)+\dfrac{u^2a^2e^2}{32}J_3(U)}\right)u^2a^2\beta^2$$

$$+wa(1-e^2)^{1/2}\left(\frac{K_1'(W)+\dfrac{w^2a^2e^2}{32}K_3'(W)}{K_1(W)+\dfrac{w^2a^2e^2}{32}K_3(W)}\right)w^2a^2\beta^2=0 \qquad (27)$$

Case II: When $\psi = \frac{\pi}{2}$ and $v = 1$ in determinantal eq. (24) and expand it, we get

$$\frac{1}{u^2}\frac{Ce_1'(\xi_0,\gamma_1^2)}{Ce_1(\xi_0,\gamma_1^2)}+\frac{1}{w^2}\frac{Fek_1'(\xi_0,-\gamma_2^2)}{Fek_1(\xi_0,-\gamma_2^2)}=0 \qquad (28)$$

Again applying the approximations from eqs. (26a)–(26d) in eq. (28),

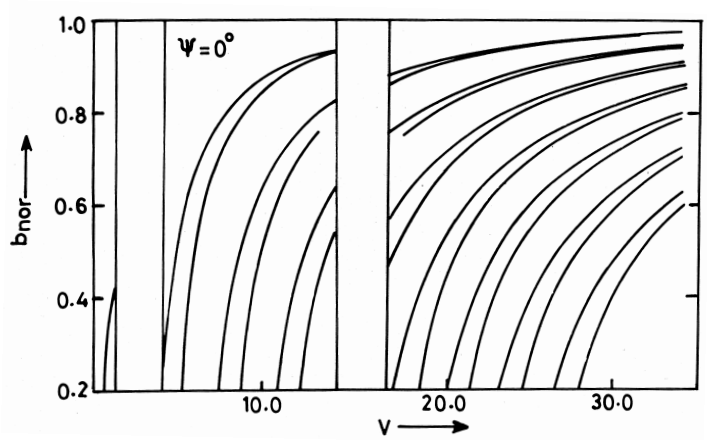

Figure 4. Dispersion curves (normalized frequency versus normalized propagation constant) for $\psi = 0°$ in the case of the elliptical step-index fiber.

we get

$$W\left[\frac{J_1'(U)+\frac{U^2e^2}{32}J_3'(U)}{J_1(U)+\frac{U^2e^2}{32}J_3(U)}\right]+U\left[\frac{K_1'(W)+\frac{W^2e^2}{32}K_3'(W)}{K_1(W)+\frac{W^2e^2}{32}K_3(W)}\right]=0 \quad (29)$$

where $U = ua$ and $W = wa$.

The dispersion curves corresponding to eq. (27) are shown in the Fig. 4. The dispersion curves corresponding to eq. (29) are shown in the Fig. 5.

5. RESULTS AND DISCUSSION

We now fix the values of ψ at $0°$ and $\frac{\pi}{2}$ for the circular step-index fiber and the elliptical step-index fiber and study dispersion curves for the sustained modes. Our core parameter is 'ua' where $u = (k^2n_1^2 - \beta^2)^{1/2}$ and 'a' is the length of the semi-major axis in the case of elliptical step-index fiber. In the case of circular step-index fiber, the size parameter 'a' is the radius of the core. The cladding parameter is 'wa' where $w = (\beta^2 - k^2n_2^2)^{1/2}$. The normalized frequency V is calculated by the common formula $V = \frac{2\pi a}{\lambda}(n_1 - n_2^2)^{1/2}$, however '$a$' has two different interpretations for the different fibers. The normalized propagation

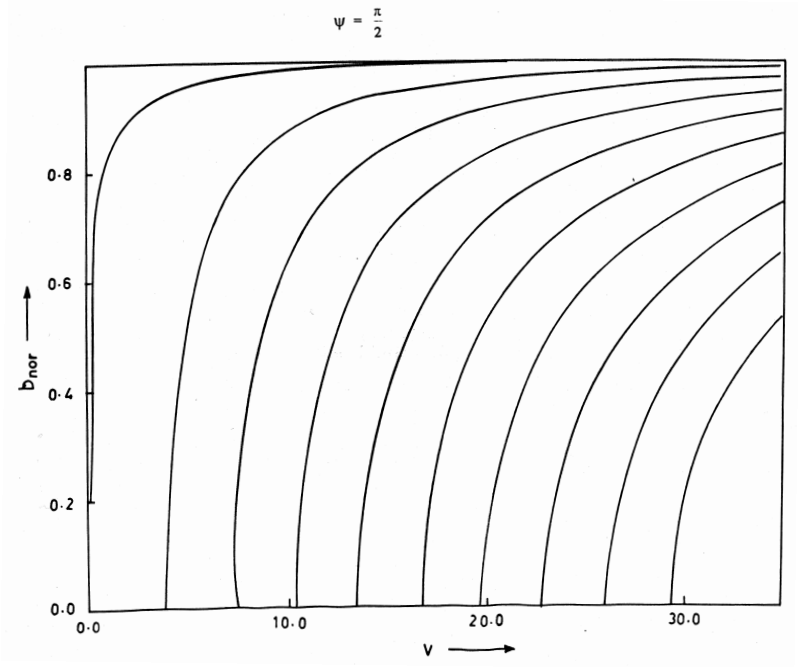

Figure 5. Dispersion curves (normalized frequency versus normalized propagation constant) for $\psi = \pi/2$ in the case of the elliptical step-index fiber.

parameter b_{nor} is obtained from the formula

$$b_{nor} = \left\{ \frac{\beta^2 - k^2 n_2^2}{k^2(n_1^2 - n_2^2)} \right\}^{1/2}$$

we have chosen $n_1 = 1.50$, $n_2 = 1.46$ and operating wavelength $\lambda = 1.55\,\mu$m for both the cases.

We first consider $\psi = 0^\circ$. For this helical pitch angle, the sheath helix degenerates into a sheath with parallel circular windings perpendicular to the axis of the fiber. This helical structure Fig. 1(d) is a periodic structure, and in this case also there is a periodicity along the axis of the fiber. We may thus expect a band gap (In the normalized frequency parameter V) for this case for both the circular and the elliptic fibers. This expectation is confirmed in both the cases, when we look at the dispersion curves for v = 1 as shown in Fig. 2 and Fig. 4. Comparing Fig. 2 and Fig. 4, we see that there is one band gap (from $V = 27$ to $V = 29$) in the case of the circular step index fiber and two band gaps (from $V = 1.3$ to $V = 4$ and $V = 14.2$ to

$V = 17$) in the elliptical step-index fiber. The band gap also occurs for much lower values of V in the case of the elliptical fiber. The effect of ellipticity is, therefore, to shift the position of the band gap to lower V-values. Other points of difference between the curves in Fig. 2 and Fig. 4 may be noted. For example, the first modal cutoff for the circular fiber is at $V = 4$, whereas the first modal cutoff for the elliptic fiber is at $V = 0.4$. This indicates that the elliptical fiber will sustain more modes for a given value of V than the circular fiber, a result which is already known for fibers without helical windings. A common feature of the curves in Fig. 2 and those in Fig. 4 is that modes occur in pairs in close proximity. It thus seems, that apart from the introduction of band gaps, the helical winding also has the effect of splitting each modes into two adjacent modes, removing degeneracy. We need not consider other obvious differences which can be readily seen by comparing Fig. 2 and Fig. 4.

We may attempt now to have a qualitative insight in to the characteristics described in the preceding paragraph. It may be pointed out here that in computing the dispersion curves, b is considered as the dependent variable and V as the independent variable. Thus for a fixed given value of V, we find a number of possible b values and we can put them in an increasing order. However, if we examine the curves in the direction of increasing V, we can identify individual dispersion curves for different modes as long as we do not come across a band gap. Beyond the band gap, the curves are again distinct. A confusing question arises: which curves on the right side (larger V) of the band gap should be considered as the extensions of the curves on the left side? On the one hand a visual survey prompts the conclusion that the dispersion curves continue unaffected as if the band gap did not exist.

Hence, it seems strange that the band gap is unable to bring about any effect on the part of the dispersion curve beyond it. In situations similar to this in other similar problems the slopes and other features of the curves on the two sides of the band gap are different. On the other hand, if we survey the diagrams Fig. 2 and Fig. 4 from the bottom to the top, numbering the curves accordingly, the correspondence between the portions of the curves on the two sides of the band gap can be made in a different way, and the band gap influences the dispersion by a discontinuous drop of the b value as one crosses the gap. This seems to be physically more possible. What we can say with some degree of confidence, however, is this. In the first allowed band there is only one mode in the elliptic fiber Fig. 4, in the second allowed band as many as six in the region immediately preceding the second band gap ($V \approx 14$) and in the third allowed band, immediately beyond the second band

gap, as many as eight modes Fig. 4. The band gaps, therefore, abruptly change the number of sustained modes as one crosses them; this is a physically acceptable result.

We now come to the case $\psi = \pi/2$. In this case the sheath helix degenerates in to a sheath made of conducting lines parallel to the axis along the core-cladding boundary surface. Thus there is no periodicity in the direction of propagation and we can not expect any band gap. This is confirmed when we look at Fig. 3 and Fig. 5 which are both for the case $v = 1$. We find that the effect of ellpticity here is to shift the curves towards lower V-values. Thus for $V = 9$, (say) there is only one mode for the circular fiber and as many as three modes for the elliptic fiber. Here again, the effect of ellipticity is to increase the number of sustained modes for a given value of V.

We may thus conclude:

1. The effect of ellipticity is to increase the number of modes for a given values of V, which is also true for fibers without winding.
2. The effect of helical conducting winding is to introduce band gaps in V-values, and as one crosses a band gap there is an abrupt change in the number of sustained modes.
3. Another effect of the conducting helical winding is to split a mode into a pair of adjacent modes. This is equivalent to removing a degeneracy of the modes.

All these results are not only theoretically interesting but also may prove to be of technical use.

ACKNOWLEDGMENT

The author is thankful to Prof. P. Khastgir, formerly of the Department of Applied Physics, Banaras Hindu University, Varanasi-221005 and K. K. Verma retired Lecturer, D.L.W. Inter College, Varanasi for their constructive and timely criticism which was of great help.

REFERENCES

1. Marcuse, D., *Theory of Dielectric Waveguides*, Academic Press, New York, 1974.
2. Adams, M. J., *An Introduction to Optical Waveguides*, 250–257, John Wiley and Sons, Chichster, England, 1981.
3. Cherin, A. H., *An Introduction to Optical Fibers*, 85–98, McGraw-Hill, New York, 1987.

4. Snyder, A. W. and J. D. Love, *Optical Waveguide Theory*, 248–255 and 311–315, Chapman and Hall, London, 1983.
5. Gloge, D., "Dispersion in weakly guiding fibers," *Appl. Opt.*, Vol. 10, 2442–2445, 1971.
6. Gloge, D., "Propagation effects in optical fibers," *IEEE Trans. Microwave Theory Tech.*, Vol. 23, 106–120, 1975.
7. Gloge, D., "Weakly guiding fibers," *Appl. Opt.*, Vol. 10, 2252–2258, 1971.
8. Chu, L. J., "Electromagnetic waves in elliptic hollow pipes of metal," *J. Appl. Phy.*, Vol. 9, 583–591, 1938.
9. Dyott, R. B. and J. R. Stern, "Group delay in glass fiber waveguides," *Electronics Letters*, Vol. 7, 82–84, 1971.
10. Singh, U. N., O. N. Singh II, P. Khastgir, and K. K. Dey, "Dispersion characteristics of a helically cIadded step-index optical filber analytical study," *J. Opt. Soc. Am. B*, 1273–1278, 1995.
11. Kumar, D. and O. N. Singh II, "Modal characteristics equation and dispersion curves for an elliptical step-index fiber with a conducting helical winding on the core-cladding boundary — An analytical study," *IEEE, Journal of Light Wave Technology*, Vol. 20, No. 8, 1416–1424, USA, August 2002.
12. Kumar, D. and O. N. Singh II, "Some special cases of propagation characteristics of an elliptical step-index fiber with a conducting helical winding on the core-cladding boundary — An analytical treatment," *Optik* Vol. 112, No. 12, 561–566, 2001.
13. Kumar, D. and O. N. Singh II, "An analytical study of the modal characteristics of annular step-index waveguide of elliptical cross-section with two conducting helical windings on the two boundary surfaces between the guiding and the non-guiding regions," *Optik*, Vol. 113, No. 5, 193–196, 2002.
14. Watkins, D. A., *Topics in Electromagnetic Theory*, John Wiley and Sons Inc., NY, 1958.
15. McLachlan, N. W., *Theory and Application of Mathieu Functions*, Oxford University Press, 1947.
16. Abramowitz, M. and I. A. Stegun, *Handbook of Mathematical Functions*, Dover Publications, New York, 1965.
17. Tai, C.-T., *Generalized Vector and Dyadic Analysis*, IEEE Press, 1992.

Deepak Kumar received the Ph.D. degree in Applied Physics from the Institute of Technology, Banaras Hindu University, Varanasi, India in 1999. He was Lecturer in Applied Physics in U.N.S, Institute of Engineering and Technology, Jaunpur,India between Nov. 2001 to May 2004. Presently he is working as a visiting Lecturer in Department of Applied physics, Delhi College of Engineering, Delhi, India. He has written two books on Mathematics one is *The Elements of Vector Algebra* and the other is *The Elements of Vector Calculus*. He has also wriffen a book on fiber-optics. His research interests include optical fibers, optical-communication, applied electromagnetic and microwave.

O. N. Singh II received the Ph.D. degree in Physics from Banaras Hindu University, Varanasi, India in 1974. Presently he is working as a Reader in Applied Physics with the Institute of Technology, Banaras Hindu University. His research interests include optical fibers, optical-communication and optical spectroscopy.